is assumed. The minimum ultimate tensile strength[14] that is acceptable for 6061 aluminum alloy in the T6 condition is 2.9×10^9 dynes/cm² (see Appendix). The compressive strength should be slightly higher than the tensile strength. The magnitude of this difference cannot be stated unequivocably until more accurate values of the relaxation are established experimentally. It is significant, however, that damage to aluminum via hypervelocity impact with the formation of hemispherical craters can be related to the tensile strength established by standard metallurgical techniques.

Work is performed on both the impacting particle and the target in an inelastic impact. This work is derived from the decay of energy of relative motion. As a metal target is deformed (penetrated) it will resist penetration.

Pertinent equations are summarized as follows:

$$P = F/A \tag{1}$$

$$Fd = W = 1/2mv^2 = \mathrm{KE} \tag{2}$$

If the product of pressure and the surface area of the crater is constant throughout the process of crater formation, then the equations for uniformly accelerated (decelerated) rectilinear motion apply:

$$F = ma \tag{3}$$

$$v^2 = 2\ ad \tag{4}$$

Combining Eqs. (1, 3, and 4), it is seen that the maximum penetration in the target is given by the following expression:

$$d = mv^2/2AP \tag{5}$$

A commonly used form of the penetration equation may be derived from uniform acceleration equations if a hemispherical crater is formed. This equation takes the form

$$d/d' = \mathrm{const}(\rho_P/\rho_T)^{1/3}(v_P/C_T)^{2/3} \tag{6}$$

where the penetration depends on the one-third power of the density ratio and the two-thirds power of the velocity ratio.

The impact of a steel projectile on an aluminum target produces a cavity whose depth approximately is equal to its diameter. Impact velocity was 4.2×10^5 cm/sec. This formation of nonhemispherical craters, impact of steel on aluminum, leads to data that do not correlate with the damage model proposed. One possible explanation for this apparent anomalous behavior may be that the steel projectile provides more resistance to flow (less viscous) than projectiles of nylon, glass, and aluminum under the conditions that prevail under impact.

Appendix

Four tensile specimens were fabricated from 6061-T6 aluminum plate used as targets in this series of tests. The experimental ultimate tensile strengths were as follows:

1) Transverse, 2.8216×10^9 dynes/cm².
2) Transverse, 3.1265×10^9 dynes/cm².
3) Longitudinal, 3.0605×10^9 dynes cm².
4) Longitudinal, 2.8802×10^9 dynes/cm².

References

[1] Bridgman, P. W., *The Physics of High Pressure* (G. Bell and Sons, Ltd., London, 1949), Chap. XIII.

[2] Bridgman, P. W., *Studies in Large Plastic Flow and Fracture* (McGraw-Hill Book Co. Inc., New York, 1952), Part I.

[3] Clark, D. S. and Wood, D. S., "The time delay for initiation of plastic deformation at rapidly applied constant stress," Am. Soc. Testing Mater. Proc. **49,** 717–735 (1949).

[4] Wood, D. S. and Clark, D. S., "The influence of temperature upon the time delay for yielding in annealed mild steel," Trans. Am. Soc. Metals **43,** 571–586 (1951).

[5] Kramer, I. R. and Maddin, R., "Delay time for the initiation of slip in metal single crystals," J. Metals **4,** 197–203 (1952).

[6] Clark, D. S. and Wood, D. S., "The tensile impact properties of some metals and alloys," Trans. Am. Soc. Metals **42,** 45–74 (1950).

[7] Ginns, D. W., "The mechanical properties of some metals and alloys broken at ultra-high speeds," J. Inst. Metals **61,** 61–78 (1937).

[8] Bridgman, P. W., "Effects of high hydrostatic pressure on the plastic properties of metals," Rev. Mod. Phys. **17,** 3–14 (1945).

[9] Kolsky, H. and Shearman, A. C., "Investigation of fractures produced by transient stress waves," Research **2,** 384–389 (1949).

[10] Rinehart, J. S., "Discussion of paper by D. S. Wood: 'On longitudinal plane waves of elastic-plastic strain in solids,'" J. Appl. Mech. **20,** 307–308 (1953).

[11] Gehring, J. W., Jr., "Observations of the phenomena of hypervelocity impact," Fourth Hypervelocity Impact Symposium, APGC-TR-60-39 (II), Paper 29 (September 1960).

[12] Rinehart, J. S., "Some observations on high-speed impact," Popular Astron. **58,** 458–464 (1950).

[13] Rinehart, J. S. and Pearson, J., *Behavior of Metals Under Impulsive Loads* (The American Society for Metals, Cleveland, Ohio, 1954), Chap. XII.

[14] *Strength of Metal Aircraft Elements,* Military Handbook-5 (March 1959), Chap. III.

Triangular Plate Elements in the Matrix Force Method of Structural Analysis

J. S. Przemieniecki*
Air Force Institute of Technology, Wright-Patterson Air Force Base, Ohio

The flexibility properties for the triangular plate element are derived for a set of three independent force systems acting along the three sides of the triangle. These systems lead to very simple patterns for the self-equilibrating (redundant) force systems which may be used in the matrix force method of analysis of structures with triangular plates. The flexibility and relative thermal displacement matrices derived for these force systems can be included in the subroutine library of flexibility properties in any of the computer programs for the analysis of complex structures.

Introduction

The use of triangular plates as basic elements in matrix structural analysis is very attractive since such elements can be employed in the idealization of nonorthogonal panels. The triangular plate elements so far have been used mainly in the displacement method of analysis[1] in which the element forces on the triangular plates are related to the corresponding displacements through the stiffness matrices determined on the assumption of linearly varying displacements. This assumption leads to a compatible constant stress field that also satisfies the stress equilibrium equations within the triangle. Since the stresses vary from element to element there is, in general, a discontinuity in stress distribution across the boundaries of adjacent elements violating the boundary equilibrium. The satisfaction of overall equilibrium of the complete stress field is then achieved through the equilibrium of equivalent element forces at common joints.

The concept of constant stress field in triangular plates also can be applied to the matrix force method of analysis.

Received by IAS December 10, 1962; revision received June 3, 1963.

* Associate Professor and Acting Head, Department of Mechanics. Associate Fellow Member AIAA.

This leads to the formulation of flexibility properties of triangular plate elements that can be used in the analysis of three-dimensional structures comprising not only triangular plate elements but also other elements such as bars, shear panels, and beams.[2–4] The flexibility properties for a triangular plate element of constant thickness will be derived here by the application of the Unit Load Theorem[4] to a set of three independent force systems acting along the three sides of the triangle.

Independent Force Systems

The element force-stress relationship based on the assumption of linearly varying displacements (or constant stress field) in the triangular plate shown in Fig. 1 is given by the matrix equation[1]:

$$\begin{bmatrix} F_1 \\ F_2 \\ F_3 \\ F_4 \\ F_5 \\ F_6 \end{bmatrix} = \frac{t}{2} \begin{bmatrix} y_{32} & 0 & -x_{32} \\ 0 & -x_{32} & y_{32} \\ -y_{31} & 0 & x_{31} \\ 0 & x_{31} & -y_{31} \\ y_{21} & 0 & -x_{21} \\ 0 & -x_{21} & y_{21} \end{bmatrix} \begin{bmatrix} \sigma_x \\ \sigma_y \\ \sigma_{xy} \end{bmatrix} \tag{1}$$

where t represents the plate thickness (assumed to be constant) and

$$x_{ij} = x_i - x_j \qquad y_{ij} = y_i - y_j \qquad i, j = 1, 2, 3 \tag{2}$$

Out of the six forces $F_1 \ldots F_6$ acting at the vertices of the triangular plate, only three force systems are linearly independent, because the six forces obviously must be related by three equations of overall equilibrium. Three independent sets of four forces, one applied force and three reactions, could be selected but their selection would be dependent on the orientation of the triangle and, in general, it would be different for each element. This situation can be avoided by selecting three sets of edge forces S_1, S_2, and S_3, as shown in Fig. 1; these forces are independent from one another and they are related to the forces $F_1 \ldots F_6$ by the matrix equation:

$$\begin{bmatrix} F_1 \\ F_2 \\ F_3 \\ F_4 \\ F_5 \\ F_6 \end{bmatrix} = \begin{bmatrix} -l_{12} & 0 & l_{31} \\ -m_{12} & 0 & m_{31} \\ l_{12} & -l_{23} & 0 \\ m_{12} & -m_{23} & 0 \\ 0 & l_{23} & -l_{31} \\ 0 & m_{23} & -m_{31} \end{bmatrix} \begin{bmatrix} S_1 \\ S_2 \\ S_3 \end{bmatrix} \tag{3}$$

where l_{ij} and m_{ij} denote direction cosines for the direction along the edge ij.

If only S_1 forces are applied, then the stresses due to this force system can be determined from Eqs. (1) and (3). Hence,

$$\sigma_x = 2l_{12}^2 S_1/th_3 \qquad \sigma_y = 2m_{12}^2 S_1/th_3$$
$$\sigma_{xy} = 2l_{12}m_{12}S_1/th_3 \tag{4}$$

where h_3 denotes the triangle height measured from the vertix 3.

It can be demonstrated easily that Eqs. (4) represent, in fact, a constant stress:

$$\sigma_{12} = 2S_1/th_3 \tag{5}$$

in the direction of the edge 1, 2. By cyclic changes of suffices in Eqs. (4), stresses due to S_2 and S_3 can be obtained. Combining the stress equations into a single matrix equation the following stress-force relationship is obtained:

$$\begin{bmatrix} \sigma_x \\ \sigma_y \\ \sigma_{xy} \end{bmatrix} = \frac{2}{t} \begin{bmatrix} l_{12}^2/h_3 & l_{23}^2/h_1 & l_{31}^2/h_2 \\ m_{12}^2/h_3 & m_{23}^2/h_1 & m_{31}^2/h_2 \\ l_{12}m_{12}/h_3 & l_{23}m_{23}/h_1 & l_{31}m_{31}/h_2 \end{bmatrix} \begin{bmatrix} S_1 \\ S_2 \\ S_3 \end{bmatrix} \tag{6}$$

or, symbolically in matrix notation,

$$\boldsymbol{\sigma} = \mathbf{a}\,\mathbf{S} \tag{6a}$$

where meaning of the matrix symbols is evident from Eq. (6).

Flexibility and Thermal Displacement Matrices

The element relative displacement-force relationship can be determined most conveniently by the application of the Unit Load Theorem[4] which states that the relative displacements corresponding to the forces $\mathbf{S}$ can be calculated from

$$\mathbf{v} = \begin{bmatrix} v_1 \\ v_2 \\ v_3 \end{bmatrix} = \int_v \bar{\boldsymbol{\sigma}}'\, \mathbf{e}\, dV \tag{7}$$

where $\bar{\boldsymbol{\sigma}}$ represents the matrix of statically equivalent stresses due to unit loads in the directions of $\mathbf{S}$, and $\mathbf{e}$ represents the exact strains. Since $\mathbf{e}$ is not known it may be assumed, as an approximation, that the strains $\mathbf{e}$ are derived from the constant stress field $\boldsymbol{\sigma}$.

The strain-stress relationship for thin plates is given by

$$\mathbf{e} = \begin{bmatrix} e_x \\ e_y \\ e_{xy} \end{bmatrix} = \frac{1}{E} \begin{bmatrix} 1 & -\nu & 0 \\ -\nu & 1 & 0 \\ 0 & 0 & 2(1+\nu) \end{bmatrix} \begin{bmatrix} \sigma_x \\ \sigma_y \\ \sigma_{xy} \end{bmatrix} + \alpha T \begin{bmatrix} 1 \\ 1 \\ 0 \end{bmatrix} \tag{8}$$

where E is the Young's modulus, ν is the Poisson's ratio, α is the coefficient of thermal expansion, and T is the temperature change. For subsequent calculations, however, Eq. (8) will be expressed in matrix form as

$$\mathbf{e} = \mathbf{C}\,\boldsymbol{\sigma} + \mathbf{B}\,\alpha T \tag{8a}$$

From Eq. (6a) it is evident that $\bar{\boldsymbol{\sigma}}$ can be taken as

$$\bar{\boldsymbol{\sigma}} = \mathbf{a} \tag{9}$$

Substituting Eqs. (6a, 8a, and 9) into (7), it follows that,

$$\mathbf{v} = \mathbf{f}\mathbf{S} + \mathbf{H} \tag{10}$$

where

$$\mathbf{f} = \int_v \mathbf{a}'\,\mathbf{C}\,\mathbf{a}\, dV \tag{11}$$

represents the element flexibility matrix and

$$\mathbf{H} = \alpha T \int_v \mathbf{a}'\,\mathbf{B}\, dV \tag{12}$$

represents the relative thermal displacements for $\mathbf{S} = 0$. Multiplying out matrices in Eqs. (11) and (12) and then integrating over the whole volume of the element, it can be shown that $\mathbf{f}$ and $\mathbf{H}$ may be expressed as

$$\mathbf{f} = \frac{2}{\mathrm{Et}} \begin{bmatrix} \sin\theta_3/\sin\theta_1 \sin\theta_2 & (\cos\theta_2 \cot\theta_2 - \nu \sin\theta_2) & (\cos\theta_1 \cot\theta_1 - \nu \sin\theta_1) \\ (\cos\theta_2 \cot\theta_2 - \nu \sin\theta_2) & \sin\theta_1/\sin\theta_2 \sin\theta_3 & (\cos\theta_3 \cot\theta_3 - \nu \sin\theta_3) \\ (\cos\theta_1 \cot\theta_1 - \nu \sin\theta_1) & (\cos\theta_3 \cot\theta_3 - \nu \sin\theta_3) & \sin\theta_2/\sin\theta_3 \sin\theta_1 \end{bmatrix} \tag{13}$$

and

$$\mathbf{H} = \alpha T \begin{bmatrix} s_{12} \\ s_{23} \\ s_{31} \end{bmatrix} \tag{14}$$

where θ_1, θ_2, and θ_3 are the triangle angles shown in Fig. 1, and s_{12}, s_{23}, and s_{31} represent the lengths of the three sides of the triangle. It is interesting to note that the relative thermal displacements $\mathbf{H}$ represent simply elongations of the three sides of the triangle due to the temperature change T, as it could be expected from physical reasoning.

Self-Equilibrating Force Systems

The structural idealization based on the concept of constant stress in triangular plate elements can be represented by a two-dimensional pin-jointed framework made up by the

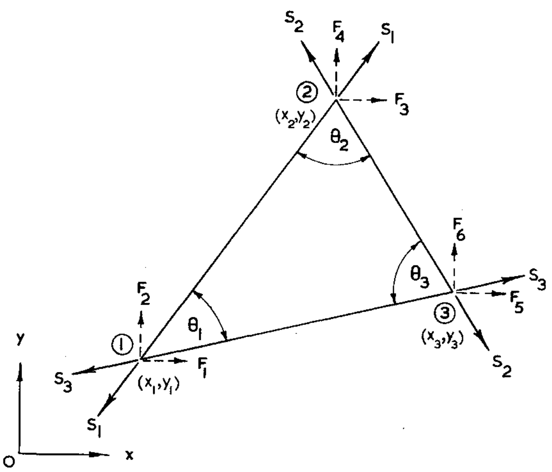

Fig. 1 Independent force systems S = $\{S_1S_2S_3\}$ on a triangular plate element.

sides of triangular elements such that when adjacent sides of two triangular plate elements meet, the corresponding framework elements are represented by two parallel pin-jointed bars. However, in contrast to a real pin-jointed framework, where the flexibility of each unassembled bar element is independent of other elements, the flexibilities of bar elements in the idealized framework are coupled in sets of three bars representing the three sides of a triangular plate element.

The self-equilibrating (redundant) force systems in the idealized structure can be interpreted as sets of forces arising from unit forces acting across fictitious cuts that are selected in such a way that the idealized structure is reduced to a statically determinate one. These systems form simple patterns in a structure made up by triangular plate elements. Some such systems for two-dimensional structures are shown in Fig. 2. The two-element systems consist simply of a pair of S forces belonging to two adjacent triangular elements (Fig. 2a). Systems involving three or four triangular plate elements are shown in Figs. 2b and 2c. Naturally, systems comprising more than four elements also can be constructed.

a) 2-element system

b) 3-element system

c) 4-element system

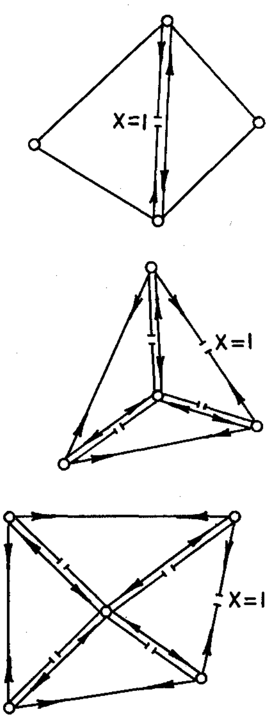

Fig. 2 Self-equilibrating force systems in triangular plate elements (two-dimensional structures).

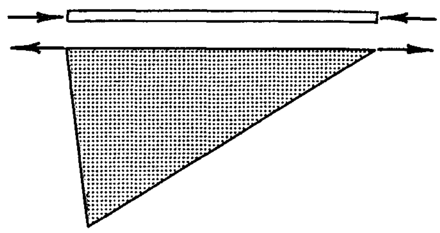

Fig. 3 Self-equilibrating force system consisting of a triangular plate and edge stiffener.

The two-element system can be used even if two adjacent plates are inclined. Furthermore, a system comprising only one triangular plate element and a bar element can be constructed as shown in Fig. 3. Complex three-dimensional structures, however, would require other types of self-equilibrating systems which can be best generated from the equations of equilibrium for the element forces S.

References

[1] Turner, M. J., Clough, R. W., Martin, M. C., and Topp, L. J., "Stiffness and deflection analysis of complex structures," J. Aeronaut. Sci. **23,** 805–823, 854 (1956).

[2] Denke, P. H., "A matrix method of structural analysis," *Proceedings of the Second U. S. National Congress of Applied Mechanics* (American Society of Mechanical Engineers, New York, June 1954), pp. 445–451.

[3] Crichlow, W. J. and Haggenmacher, G. W., "The analysis of redundant structures by the use of high-speed digital computers," J. Aerospace Sci. **27,** 595–606, 614 (1960).

[4] Argyris, J. H., "Energy theorems and structural analysis," Aircraft Eng. **26,** 347–356, 383–387, 394 (1954); **27,** 42–58, 80–94, 125–134, 145–158 (1955); also reprinted by Butterworths Scientific Publications, London (1960).

A Property of Optimum Paths Common to Newtonian and Uniform Force Fields

MAURICE L. ANTHONY* AND FRANK T. SASAKI†
Martin Company, Denver, Colo.

THIS paper is concerned with the path of a vehicle which is required to pass through two prescribed points, P_1 and P_2, as shown in Fig. 1. For a given force field, this requirement imposes a relation between the speed and direction of motion at P_1. Three force fields are studied: 1) the Newtonian or inverse square force field, 2) the uniform parallel force field, and 3) the linear central force field. In each field the path is found for which the speed V_1 is a minimum. For the first two fields, which are used most often in preliminary analyses, it is shown that the associated flight path angles are identical. A study of the third field shows that this result is not true for general radially dependent central force fields.

In a Newtonian force field the vehicle path is determined in terms of the initial conditions by the following equations:

$$u'' + u = \mu/r_1^2V_1^2 \cos^2\alpha_1 \tag{1a}$$

and at $\theta = \theta_1 = 0$,

$$\begin{aligned} u &= 1/r_1 \\ u' &= -(1/r_1)\tan\alpha_1 \end{aligned} \tag{1b}$$

where $u = 1/r$, a prime indicates differentiation with respect

Received December 21, 1962.

* Manager, Astrodynamics Staff. Associate Fellow Member AIAA.

† Assistant Research Scientist. Member AIAA.